13th World Conference on Earthquake Engineering
Vancouver, B.C., Canada
August 1-6, 2004
Paper No. 1664

SIMULATION OF BRICK MASONRY WALL BEHAVIOR UNDER IN-PLANE LATERAL LOADING USING APPLIED ELEMENT METHOD

Bishnu Hari PANDEY[1], Kimiro MEGURO[2]

SUMMARY

Failure of masonry buildings is considered as the major cause of the large number of casualties during the past earthquakes around the world. Masonry constructions are still in practice even in highly seismic regions. Understanding of masonry wall behavior under lateral load is important to develop proper mitigation measures applied to existing buildings for retrofitting and to new construction for setting of design guidelines. In this paper, attempt is made to apply a newly developed numerical tool, Applied Element Method (AEM), for the analysis of masonry building structures with detailed failure process comprising crack occurrences, their evolution, block separation and material loss before collapse. The study gives an insight into the failure mechanics, which is important, not only for the strength assessment, estimation of maximum dissipation level and collapse, process, but also for the identification of weak point locations, their extent and force transfer paths. Performance of the application of AEM is evaluated with available experimental results of masonry wall under in-plane cyclic loading. Comparison is made between observed behavior in experiment and numerical prediction for crack pattern, their evolution and hysteretic behavior. Application is further extended to numerical simulation of walls under different configurations to observe the effect of wall aspect ratio, opening locations and their size and boundary conditions.

INTRODUCTION

Masonry is being used as a major structural material for building construction in most of the developing countries. Despite its long traditional use, past and recent experiences have shown that masonry buildings have poorly performed during earthquakes leading to complete collapse of the structures and great number of casualties [EERI, 1, EERI, 2]. The construction is still in practice even in highly seismic regions. Understanding of masonry wall behavior under lateral load is important in evaluating the seismic vulnerability of existing buildings and, so, to develop proper retrofitting measures. The proper estimation of wall behavior can also be applied to new construction for setting of design guidelines.

Masonry sustains damage in form of cracks in early stage of loading as the mortar break in a low level of load compared to brick units. Unlike in the reinforced concrete where cracks can signify to vulnerability to collapse, onset of cracking along the mortar joints in masonry is indication of inelastic response rather than failure

[1] Earthquake Engineer, NSET, Kathmandu, Nepal. Email: bpandey@nset.org.np
[2] Professor, IIS, University of Tokyo, Tokyo, Japan. Email: meguro@iis.u-tokyo.ac.jp

[Langenbach, 3]. Masonry works well after the first cracking allowing frictional sliding which contribute to energy dissipation. During this process, there could be large displacement discontinuity between the blocks without much loss in strength. The phenomenon takes place in framed masonry more vividly as panel sustain cracks in early loading but held in place by the confining action of surrounding frame. Earthquake resistance mechanism lies on stability given by the frame that can act in linear range while adjacent masonry panel allow the excess energy dissipation. In cyclic loading case, separation of wall panel in tension and recontact in compression in successive cycle accommodate large displacement. It is needed in analysis to capture this local behaviour to represent the overall response of wall in simulation.

In micro-level modelling of masonry, attempts have been made to implement it in Finite Element Method (FEM) of numerical analysis through smeared crack approach [Lofti et al, 4] and discrete approach with use of interface elements [Page, 5, Lourenco et al, 6]. Research has been done with use of Discrete Element Method to analyse the masonry composed of block units [Lemos, 7]. In Finite Element analysis with smeared model problem of mesh sensitivity, failure to capture diagonal shear have been identified [Lofti et al, 4] where as FE analysis using interface model overcomes the problems. However, it requires a special treatment for interface element and is time consuming for the analysis of wall structure. Discrete Element Method can deal easier with large displacement and total separation of the bodies. However, poor constitutive laws for brick and interface are used to deal with large collection of blocks. Computational cost in analysis may become very high in this case.

To this end, Applied Element Method (AEM) is regarded as a numerical tool capable to follow the complete structural response until total degradation in large displacement range with reasonable accuracy [Meguro et al, 8]. So far, AEM has been used to simulate the behaviour of concrete and soil [Ramancharla, 9]. However, its applicability to the structures composed of blocky masonry units is realized by the features: (i) Element formulation in AEM to discretize the structure into small virtual elements can trace the exact mapping of masonry unit laying with mortar joint location and (ii) It allows large displacement between elements and analysis of structure with separated parts after large cracks is possible with reasonable accuracy. Bonding of rigid brick units by mortar in interfaces in masonry wall can be well characterized by element connectivity in AEM

In this paper, Applied Element simulation of clay brick masonry wall under in-plane lateral load is discussed. Masonry is discretized such that brick units are represented by number of small elements with mortar joint at their corresponding edges. Principal stress failure criterion is used for units and Mohr-Coulomb's friction model with tension cut-off is implemented to model interface behavior including mortar. Formulation of softening in the process of loss of cohesion and debonding is applied to describe the shear behavior in tensile regime. Performance of current application of AEM is evaluated with available experimental result of a wall with opening under monotonic lateral load. Comparison is made between observed behavior in experiment and numerical prediction for crack pattern, their evolution and load-displacement relation.

APPLED ELEMENT MODELLING OF MASONRY

In AEM, structure is assumed to be virtually divided into small square elements each of which is connected by pairs of normal and shear springs set at contact locations with adjacent elements. These springs bear the constitutive properties of the domain material in the respective area of representations (Fig. 1). Global stiffness of structure is built up with all element stiffness contributed by that of springs around corresponding element. Global matrix equation is solved for three degrees of freedom of these elements for 2D problem. Stress and strain are defined based on displacement of spring end points of element edges. Details of Applied Element scheme can be found in literatures, for instance, Meguro et al. [8].

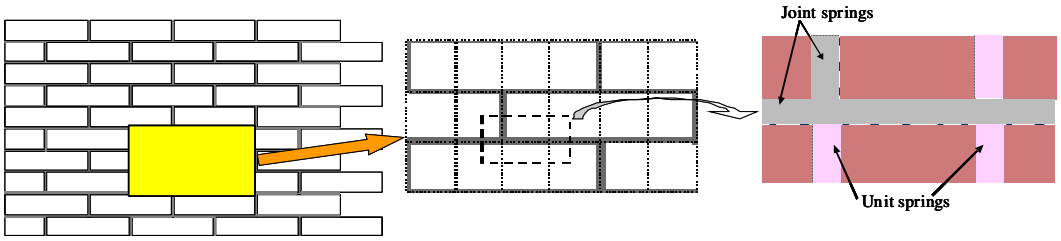

(a) Masonry wall (b) Closer view (c) Joint detail

Fig. 1 Masonry discretization

As AEM so far has been used for homogeneous media like concrete and soil, to develop an application of it for multi-phase heterogeneous blocky material like masonry, it requires development of some technique that can address the particular features of masonry. Within the broad frame work of analysis process, some flexibility has been added in problem statement, mesh generation, stiffness assignment to springs, adjustment for compatibility of plastic strain characterized by the hydro-static pressure dependent failure envelop of blocky materials, treatment of different failure modes that may be either within the different constituent material or on their interfaces. The flow as shown in chart 1 has been applied for the solution.

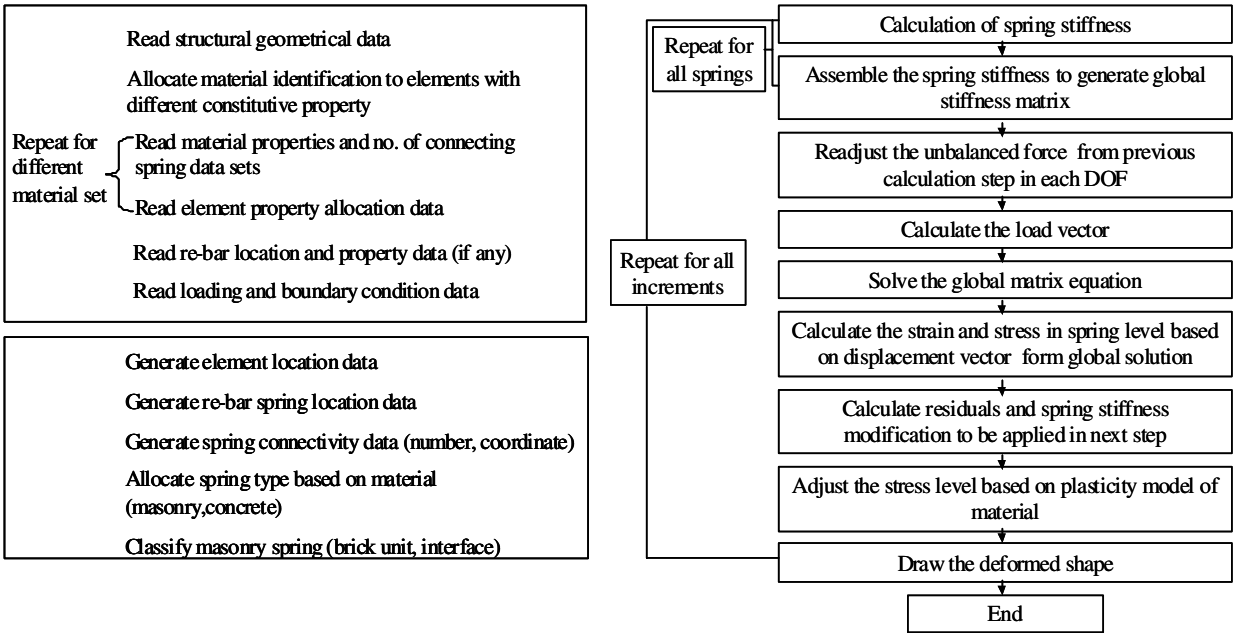

(a) Input and discritization (b) Analysis

Chart 1 Flow chart of AEM numerical analysis for masonry

Descritization for brick masonry

To take the account of anisotropy of masonry, which is two-phase material with brick units and mortar joints set in a regular interval, structure is discretized such that each brick unit is represented by a set of square elements where mortar joints lie in their corresponding contact edges. For different brick laying pattern, a scheme is developed so that portion of overlapping of upper layer brick to the immediate below one can be chosen so that desired bonding pattern could be achieved with exact location of the mortar

joint. The staggered location of head joint will be matching as to lie in contact edge of end element of each brick unit

In spring level, springs that lie within one unit of brick are termed as '*unit springs*'. For those springs, the corresponding domain material is brick as isotropic nature and they are assigned to structural properties of brick. Springs those accommodate mortar joints are treated as '*joint springs*'. They are defined by equivalent properties based on respective portion of unit and mortar thickness. Figure 1 shows the configuration of brick units, joints and their representation in this study. The initial elastic stiffness values of joint springs are defined as in Eqs. 1 and 2**.**

$$K_{nunit} = \frac{E_u \,.\, t \,.\, d}{a} \;; \qquad K_{njoint} = \frac{E_u \,.\, E_m \,.\, t \,.\, d}{E_u \;x\; t_h \;+\; E_m \;(a \;-\; t_h)} \tag{1}$$

$$K_{sunit} = \frac{G_u \,.\, t \,.\, d}{a} \;; \qquad K_{sjoint} = \frac{G_u \,.\, G_m \,.\, t \,.\, d}{G_u \,.\, t_h \;+\; G_m \;(a \;-\; t_h)} \tag{2}$$

Where E_u and E_m are Young's modulus for brick unit and mortar, respectively, whereas G_u and Gm are shear modulus for the same. Thickness of wall is denoted by t and t_h is mortar thickness. Dimension of element size is represented by a and d is the fraction part of element size that each spring represent.

While assembling the spring stiffness for global matrix generation, contribution of all springs around the structural element are added up irrespective to the type of spring. In the sense, for global solution of problem, there is no distinction of different phase of material but only their corresponding contribution to the stiffness system.

Material modelling

As discussed in last section, joint spring in this study will represent not only the mortar but also the mortar-brick interaction in those regions. Implementation of a completely separate model for mortar could be applied but element size to represent the structure in the order of mortar thickness will require large no of elements for prototype wall size. This leads to CPU time requirement very high. In this context, failure modes observed in the masonry which involves mortar or interaction of mortar and brick are to be characterized by joint springs.

Considering the major failure modes of masonry, failure occurs as: (1) cracking of the joints, (2) sliding along the bed or head joints, (3) cracking of units under direct tension, (4) diagonal tensile cracking of the units under high compression and shear, and (5) "masonry crushing", which is actually splitting of bricks. Among the failure modes, behavior of mortar joint interfaces is responsible for tension cracking with debonding (1) and friction sliding under compressive stress in joints (2) [Gambarrota et al, 10]. Coulomb's friction model with tension cut-off can represent these mechanisms. The failure modes (3) and (4) are to be described by the constitutive property of the brick springs. Tensile fracture of bricks due to different transversal deformation both in mortar joint and in the bricks is to be involved as a joint property [Crisafulli, 11].

In the direction of predicting overall behaviour of joint, some research has been done to establish the constitutive relation of interface. To include failure mode (5) without considering the interaction between mortar and brick explicitly, a compression cap can be implemented to limit the compression stresses in the masonry according to the behaviour observed under uniaxial testing. To bring all the joint related failure

under unified model, Lourenco et al [6] proposed interface model which combines a cap failure surface under high compression with tension cut-off and Coulomb's friction envelops.

In this study, composite model that takes account brick and mortar with their respective constitutive relation with elastic and plastic behaviour of hardening and softening is implemented. Brick springs are assumed to follow principal stress failure criteria with linear elastic behaviour. Once there is spitting of brick reaching elastic limit, normal and shear stress are assumed not to transfer through cracked surface in tensile state. The brick spring's failure criterion is based on a failure envelope given by:

$$\frac{f_b}{f'_b} + \frac{f_t}{f'_t} = 1 \tag{3}$$

Where f_b and f_t are the principal compression and tensile stresses, respectively, and f'_b and f'_t are the uniaxial compression and tensile strengths, respectively.

Coulomb's friction surface with tension cut-off is used as yield surface after which softening of cohesion and maximum tension takes place in exponential form as a function of fracture energy values and state variables of damage. The cohesion and bond values are constant till the stress first time when stress exceeds the respective failure envelopes. Figure 2 and 3 show the degradation scheme of bond and cohesion. Failure modes that comes from joint participation of unit and mortar in high compressive stress is considered by linearized compression cap modified by Sutcliffe et al, [12] to original ellipsoid cap proposed by Lourenco [6]**,** as shown in fig. 4. The effective masonry compressive stress used for cap mode follows hardening and softening law as shown in fig. 5. The tension cut-off, f_1, and the sliding along joints, f_2, exhibit softening behaviour whereas the compression cap experiences hardening at first and then softening. The failure surfaces used in this study derived from Lourenço [6], with some simplification are:

$$f_1(\boldsymbol{\sigma}, \kappa_1) = \sigma - f_t \exp\left(-\frac{f_t}{G_f^I}\kappa_1\right) \tag{4}$$

$$f_2(\boldsymbol{\sigma}, \kappa_2) = |\tau| + \sigma \tan(\phi_1) - c \exp\left(-\frac{c}{G_f^{II}}\kappa_2\right) \tag{5}$$

$$f_3(\boldsymbol{\sigma}, \kappa_3) = |\tau| + \tan(\phi_2)\{(\sigma_3(\kappa_3) - \sigma\} \tag{6}$$

where,

$$\sigma_3(\kappa_3) = \begin{cases} \sigma_i + (\sigma_p - \sigma_i)\sqrt{\dfrac{2\kappa_3}{\kappa_p} - \dfrac{\kappa_3^2}{\kappa_p^2}}, & \kappa_3 \le \kappa_p \\ \sigma_p + (\sigma_m - \sigma_p)\left(\dfrac{\kappa_3 - \kappa_p}{\kappa_m - \kappa_p}\right)^2, & \kappa_p < \kappa_3 \le \kappa_m \\ \sigma_r + (\sigma_m - \sigma_r)\exp\left(m\dfrac{\kappa_3 - \kappa_m}{\sigma_m - \sigma_r}\right), \quad m = 2\dfrac{\sigma_m - \sigma_p}{\kappa_m - \kappa_p}, & \kappa_m < \kappa_3 \end{cases} \tag{7}$$

where f_i is the i-th yield surface, κ_i hardening/softening parameter of i-th yield surface, f_t interface bond strength, $\sigma=\{\sigma,\tau\}^T$ stress at the spring, G_f^I and G_f^{II}, fracture energy in pure tension and shear, respectively, c interface initial cohesion, ϕ interface friction angle, C_{nn} and C_{ss} cap parameters, and σ_i, σ_p, σ_m, σ_r, κ_m, and κ_p are parameters obtained from uniaxial compression tests of masonry prisms. Associate flow rules are adopted for f_1 and f_3 whereas a non-associate flow rule is considered for f_2. The corresponding plastic potential is given by:

$$g_2 = |\tau| - c \tag{8}$$

One feature of the composite yield surface described by the previous equations is that f_1 and f_2 are coupled and exhibit isotropic hardening, i.e. κ_1 and κ_2 evolve simultaneously. This is consistent with the fact that cohesion and adhesion are related phenomena, i.e. a loss in cohesion results in a loss of adhesion and vice versa. On the other hand, f_2 and f_3 are not related, as they represent different phenomena: joint sliding and brick crushing, respectively. Therefore, κ_2 and κ_3 develop independently.

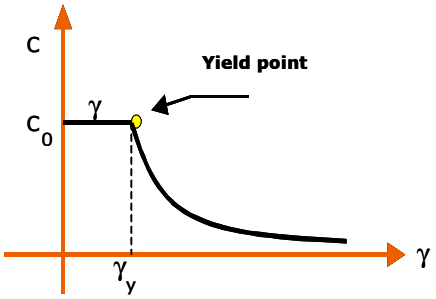

Fig. 2 Cohesion degradation

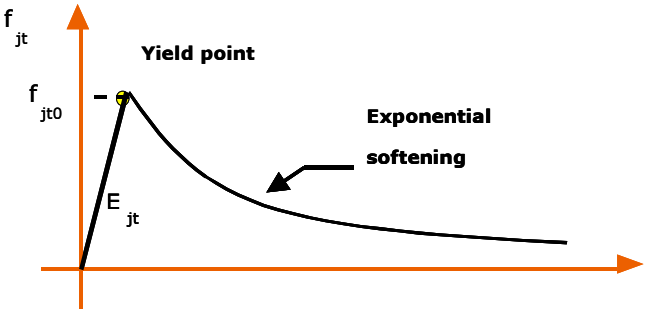

Fig. 3 Bond degradation

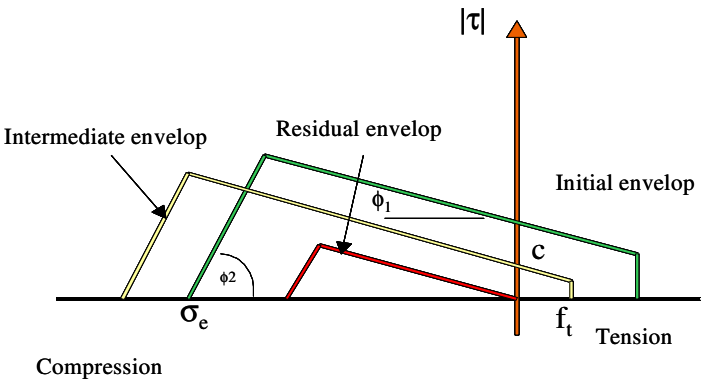

Fig. 4 Failure Criteria for joint spring

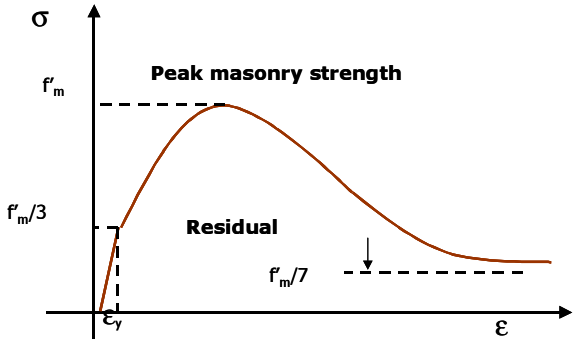

Fig. 5 Hardening and softening applied for joint spring in compression cap

Framework for Solution

After reading geometrical configuration and material property data, material property has been assigned to the corresponding elements. Springs with corresponding constituent material (brick or joint) are set to element edges after deciding the bond pattern of the brick-lying. Inputs are boundary condition and loading data where as elastic stiffness of all springs are evaluated based on Eqs. 1 and 2. Assembling all the stiffness around elements in terms of 3 degrees of freedoms at each elements centre and preparing load vector, global equations are solved. Stiffness and load vector are to be modified according to the present damage condition of springs and unbalanced force obtained from previous step solution respectively. Unbalanced forces are derived as discrepancy between maximum possible stress considering material

failure envelop and estimation of stress from global solution. The element displacements are transferred to spring ends to calculate stress and strain in local level. The obtained stress values are treated as trial stress for the plastic analysis of masonry material from which exact solution has been obtained. As the spring stiffness are set according to updated damage condition little discrepancy are expected. As the loading steps are small enough, accuracy of solution will not be affected as the unbalanced force will be applied in next step. Deformed shape of structure will be created from the current level of total displacements in each element.

WALL BEHAVIOR ANALYSIS

Simulation of wall behavior using AEM was made for experimental wall to compare between experimental observation and numerical results. As good agreement was observed between experimental results and numerical prediction the analysis was extended for walls of practical dimension to estimate the behavior under different construction and loading variables.

Experimental wall

Clay brick masonry wall with central opening test carried out by Vermeltfoort [13] is selected for analysis. It is approximately square with single wyth of brick dimension of 200 X 100 X 50 mm with 10 mm mortar thickness. Wall is subjected to vertical constant pressure of 0.3 MPa from the top. Horizontal displacement d is monotonically applied at the top layer that is clamped in steel beam. The wall and boundary condition of experimental scheme is shown in fig. 6. Material properties derived from micro-test results are reported as: brick Young's modulus, E_u = 1.67 X 104 MPa; mortar Young's modulus, E_m = 0.79 X 104 MPa; brick tensile strength, f_{ut} = 2.0 Mpa; joint tensile strength, f_{jt} = 0.25 MPa; cohesion, c = 0.35 MPa and friction angle,ϕ_1 =36.50. Masonry compressive strength f'_m is assumed as 20 Mpa and angle to define the cap mode, ϕ_2, is selected as 40^0 which lies within the application range suggested by Sutcliffie et al [12] as 20^0-70^0.

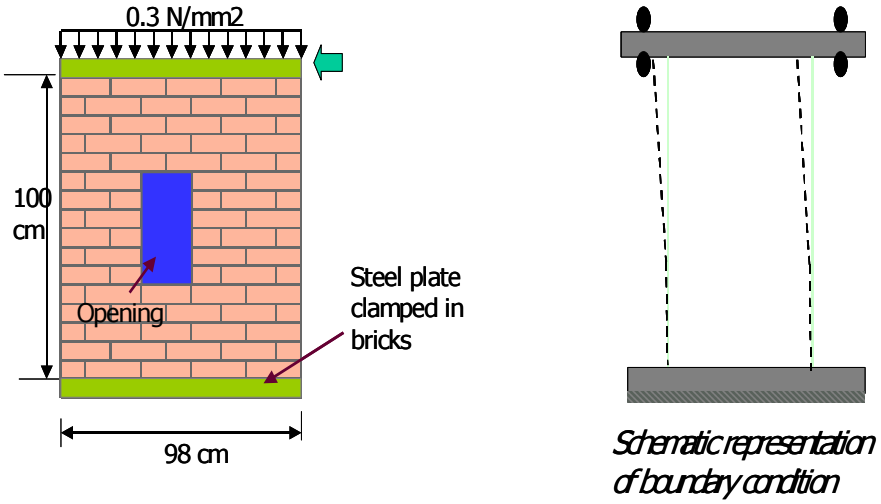

Fig. 6 Test wall and schematic boundary condition

Cracking

Cracking in wall started from very early stage of loading initiating from loaded diagonal corners of opening. The cracks propagated towards the wall corner points. However, when cracking reached vicinity of corners where enough compression has been built, further propagation stopped and new small cracks appeared at opposite wall faces. After maximum resistance was attained, those major cracks had

breakthrough along the wall diagonal. Though the cracks lie mainly in mortar regions, there is also splitting of brick units near left bottom corners. The crack location and evolution obtained by analysis agrees well with reported observation. Crack pattern observed in test and obtained through analysis are shown in figs. 7 and 8.

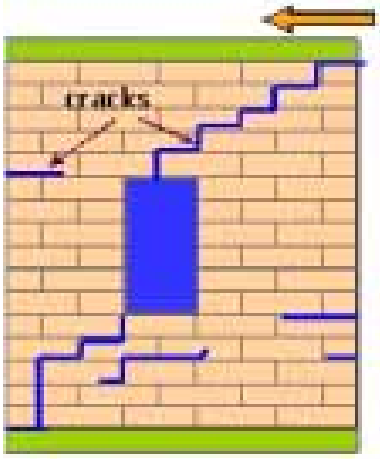

Fig. 7 Experimental crack pattern

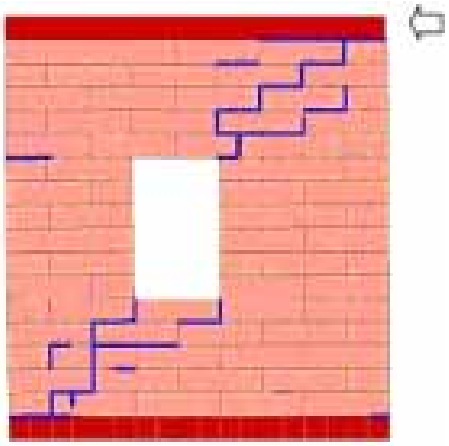

Fig. 8 Observed crack pattern from numerical simulation

Flow of Stress

Through numerical analysis, it is observed that with the increment of imposed displacement at top right corner, both compression and tension stress level increase. Compression occurs in two diagonal bands on either side of the opening as shown in fig. 8 whereas tension takes place in opposite corner locations and middle diagonal band. Initial cracking takes place in those tension spots. As load increases by virtue of increased displacement, compression stress concentration takes place in four locations as marked in fig. 9 apparently forming hinges. However, when cracks passed throughout diagonal crossing high compression zone, compression stress level does not increase and earlier high level of tension is reduced. This may be due to sliding of upper triangular part of wall over lower one through stepped cracks. In this state, energy is dissipated through sliding and wall behaves in ductile manner. Load-displacement curve as shown in fig. 10 also suggests this mechanism.

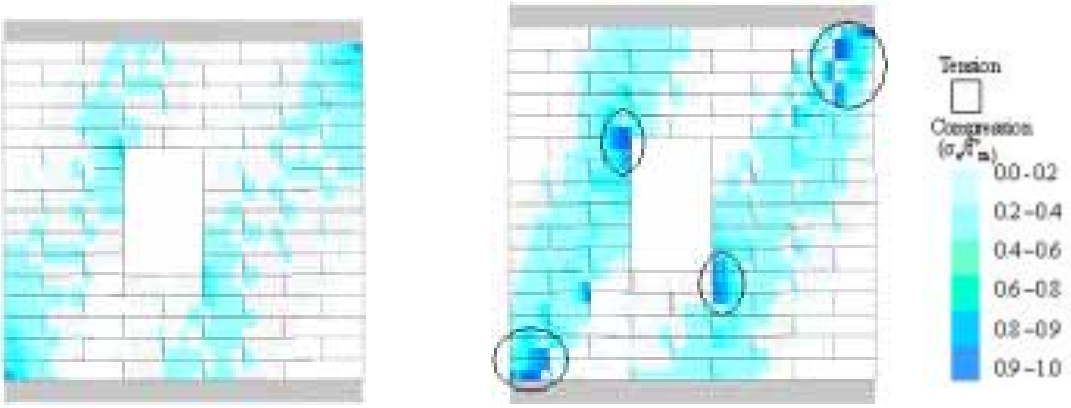

(a) at 5 mm displacement (b) at 14 mm displacement

Fig. 9 Stress distribution under lateral loading

Load-Displacement Relation

As observed in Fig. 10, earlier response is almost linear with slight deviation at 21 kN. Stiffness degradation starts when stress state lies on compression cap envelop where shear resistance is reduced with increment in compression. Sliding of upper part is represented by the flat plateau of load displacement curve. It is observed that load-displacement behaviour in experiment is well captured by numerical analysis. From these observations, it is noted that though early response of masonry shear wall is mainly due to debonding and friction sliding, reduction in shear resistance in high compression governs the peak load and post peak behaviour.

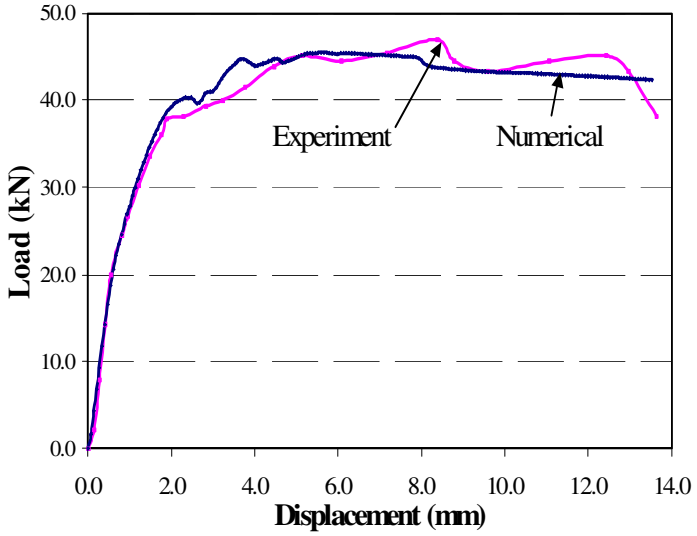

Fig. 10 Comparison of experimental and numerical analysis results

Wall with practical dimensions

The wall chosen for the numerical analysis has central doorway opening with top layer of rigid block fixed in vertical direction to represent the actual wall under rigid slab. The wall is 2.22 m high with total length of 3.0 m. The central door dimensions are 1.8 m x 0.84 m. The bricks are assumed to be laid in running bond. Material properties of masonry are as follows: brick dimensions, 240 x 120 x 60 mm, brick Young's modulus, E_u = 1.67 X 104 MPa; mortar Young's modulus, E_m = 0.79 X 104 MPa; brick tensile strength, f_{ut} = 2.0 Mpa; joint tensile strength, f_{jt} = 0.25 MPa; cohesion, c = 0.35 MPa and friction angle, ϕ_1 = 36.50. Masonry compressive strength, f'_m, is assumed as 20 Mpa and ϕ_2 selected as 40^0.

The above-mentioned physical model is descritized into 300 square elements with 4 elements for each brick unit. Element has, thus, 60 mm size. Two adjacent elements are joined using 7 connecting springs. All the elements in the bottom layer are fixed in all three degrees of freedom and the top layer is free to move in horizontal direction. Prior to the application of the lateral displacement, pre-compression load is applied to the top layer of the wall specimen. Lateral displacement of 2 cm is applied in 300 increments in positive direction of x-axis.

Behavior of wall

At the initial stages of the lateral displacement on the top layer, high tension is developed at the loaded top end of the opening simultaneously with tension at the inner bottom end of the leeward pier as shown in Fig. 11 (a). This is due to the concentration of the high compression normal to the bed joint plane along the principal diagonal. Tension patches can also be observed at the either ends of the opposite wall

corners. This concentration can be explained as the development of flexural tension. Initiation of the compression of small magnitude can also be observed at the toe and the loaded tip.

Upon increasing the lateral displacement cracks appeared first at the top left end of the opening (as shown in Fig. 11 (b)) releasing the accumulated tension to wider region. This is due to the re-distribution of the stresses by crack formation. The similar observations can be seen at other ends where the tension was concentrated. With the increase in lateral displacement further, highly compressed zones are formed at the pier corner regions approaching each other to form a diagonal band.

It is observed from the Figs. 11 (c) at 20 mm, that initial crack appeared in the corners have extended to the wall end in a stepping fashion. Damage is concentrated in a single line of stepped crack virtually separating the wall into two parts as shown in Fig. 11 (d). At the same time crack parallel to the bed joints in the mortar regions are observed both piers at the bottom zone.

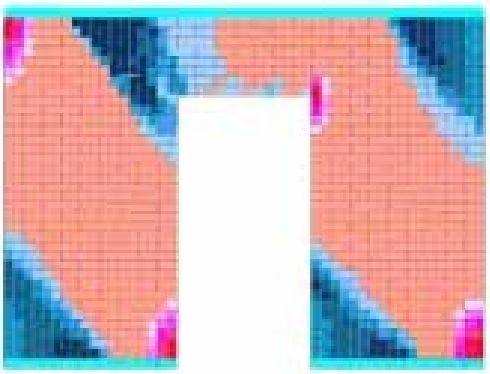

Fig 11 (a) Stress condition at 3 mm drifts

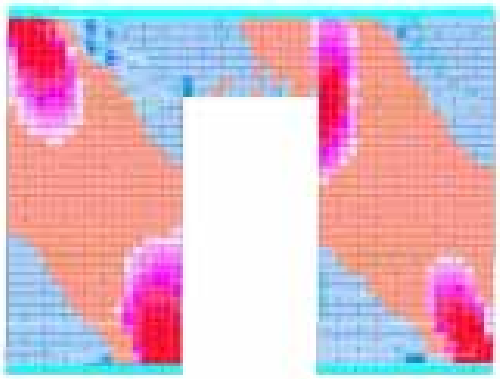

Fig 11 (b) Stress condition at 8 mm drifts

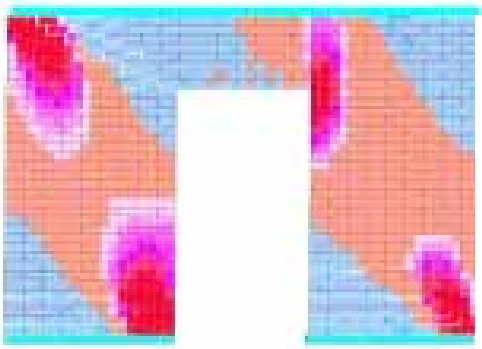

Fig 11 (c) Stress condition at 20 mm dril

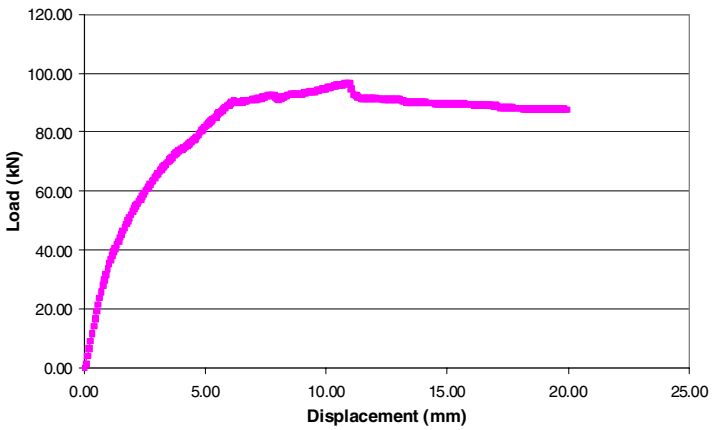

Fig 11 (d) Load displacement curve

Figure 11 (d) shows the load displacement relationship observed in the analysis. Initial wall stiffness is maintained up to 8 mm where extension of tension cracks ceased due to the adjoining compression region. Upon further loading, resistance of wall is due to the compression shear. At this stage, no new cracks except extension of the stepped cracks appeared. Once cracks pass to the corner end, little drop of the load resistance followed by constant load carrying capacity. This behaviour is characterised by the shear friction sliding of wall over left pier along crack surfaces. Displacement imposed on the specimen lead to the translatory motion of the separated block as a unit without increase in resistance. This feature can be

realised as a masonry characteristics of dissipating energy through the means of failure of mortar regions. The response of the masonry wall under the action of lateral load cannot be attributed to the single parameter but depends on various factors such as existing normal load level, material properties, construction features, etc. In this study, the following three parameters were analysed and discussed here under.

(a) Pre-compression load: For understanding the effect of the pre-compression load on the response of the masonry wall, three levels of compression load are considered i.e., no compression load, 0.84 MPa and 2.5 MPa. From the analysis results, it is observed that the increase in compression level results in the compression band formation in both piers of wall**.** Principal crack is observed in all the three cases in the same pattern. This means that the principal crack is dependent on the imposed displacement rather than on the pre-compression load. On observing the figures, we can see that more failure is concentrated in the right side pier at higher levels of compression load. Figure 12 shows the load displacement relationship of three cases. In this figure, increase in compression load is observed with increase the lateral load carrying capacity. However, this is controlled by compression cap.

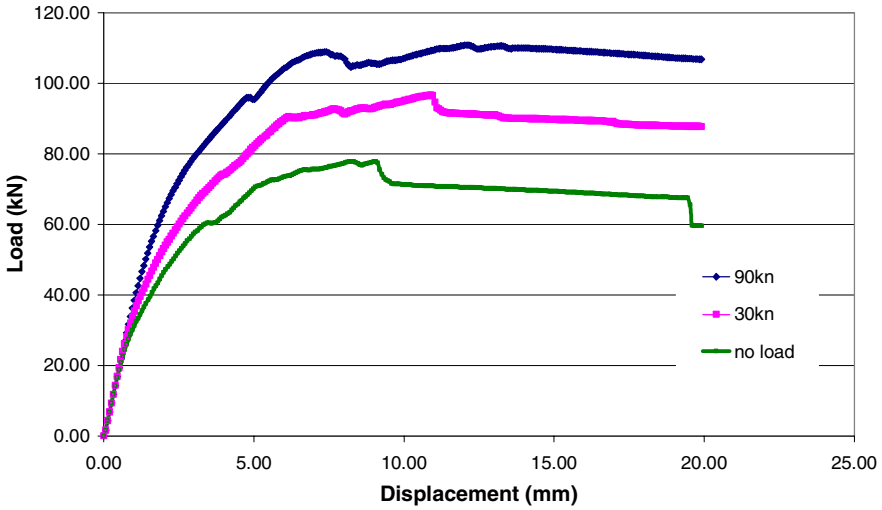

Fig. 12 Effect of pre-compression load in load –deformation relation

(b) Mortar strength

To understand the effect of mortar strength on the response of masonry wall, two different mortar strengths are considered for two levels of pre-compression loads. It is observed that the higher the mortar strength higher is the load carrying capacity all stages of loading.

(c) Lintel band

In most of the guidelines for non-engineered masonry buildings, band is recommended over the openings for better earthquake resistant performance of the buildings [IAEE, 14]. The effect of the lintel band in in-plane loading was analysed in this study by the numerical simulation. It is observed that the lintel has significant effect in wall behaviour, particularly, in crack pattern. Figures 13 (a) and 13 (b) present the positive influence of the small reinforced concrete band placed over the door opening in numerical specimen of wall. The responses of walls in both figures are at same drift level. Crack appeared in wall without band is disappeared in wall with band. The avoidance of the crack would help withstand the out of plane failure of the wall in case of transverse loading.

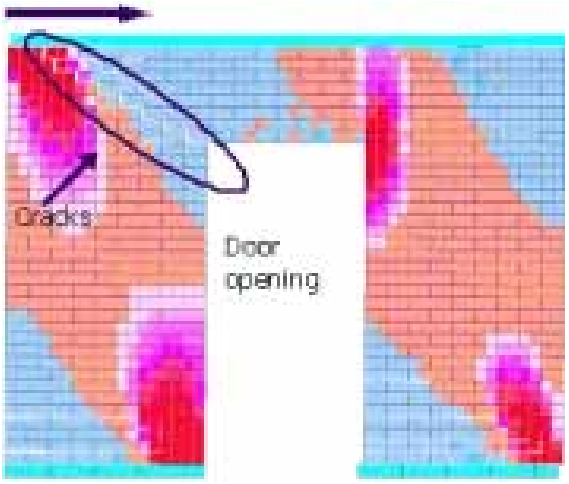

Fig. 13 (a) Crack pattern and stress distribution in wall without lintel band under lateral loading

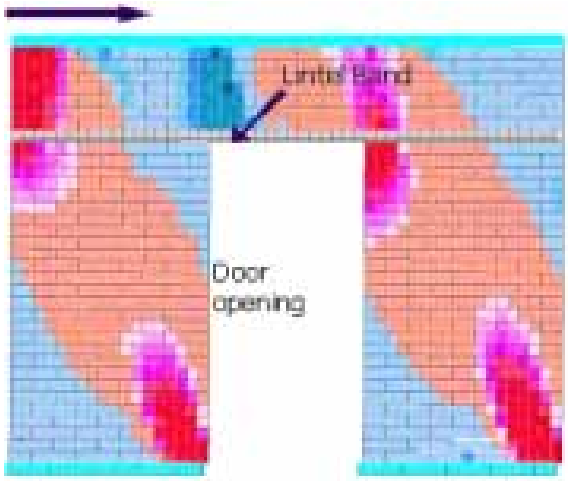

Fig. 13 (b) Crack pattern and stress distribution in wall with lintel band under lateral loading

CONCLUSION

Masonry modelling can be easily implemented in the framework of AEM. The applicability of the AEM was validated by comparison of experimental observation with numerical results. The study carried out would help understand the masonry behaviour and identify the governing factors of the complex failure process. Effects of loading condition, material characteristics and construction practice on the response have been discussed using numerical analysis results by one set of example for each case.

This study is the first attempt on the modelling of the masonry for numerical simulation using AEM. Where as it shows method's capability to capture the behaviour, further research is needed to look into the case of structure subjected to arbitrary loading path including dynamic case in both in-plane and out-pane direction. The extension of the study to reinforced masonry wall under pertaining parameters could help in guidelines of masonry retrofitting.

REFERENCES

1. EERI "Earthquake in Gujarat India: Preliminary Reconnaissance Report." EERI Special Earthquake Report, 2001.
2. EERI "Earthquake in Western Iran: Preliminary Reconnaissance Report." EERI Special Earthquake Report, 2002.
3. Langenbach R. "Earthquakes: A new look at cracked masonry." Civil Engineering, ASCE, Nov.1992: 56-58.
4. Lofti HR., Singh PB. "An appraisal of smeared crack models for masonry shear wall analysis." Computer and Structures 1991; 41(3):413-25.
5. Page AW, "Finite Element model for masonry." J. Struct. Eng. (ASCE) 1978; 104(8): 1267-85.
6. Lourenco PB, Rots JG, "Multi surface interface model for analysis of masonry structures." J. Eng. Mech. (ASCE) 1997; 123(7): 660-68.
7. Lemos JV, "Discrete element modeling of the seismic behavior of stone masonry arches." Middleton J, Pande GN, Krajl B, Editors. Computer methods in structural masonry (4). E & FN Spon, London, 1997: 220-27.

8. Meguro K, Tagel-Din H. "Applied Element Simulation of RC Structures under Cyclic Loading." Journal of Structural Engg. 2001;127(11):1295-1305.
9. Ramancharla PK. "Numerical analysis of the effects on the ground surface due to seismic base fault movement." Ph.D. thesis, Civil Eng. Dept., University of Tokyo, 2001.
10 Gambarrotta L, Lagomarsino S."Damage Model for the Seismic Response of Brick masonry Shear Wall. Part I: The Mortar Joint Model and its Applications." Earthquake Engineering and Structural Dynamics 1997; (26): 423-39.
11 Crisafulli FJ. "Seismic Behavior of Reinforced Concrete Structures with Masonry Infills." Ph.D. thesis, Dept. Civil Eng., University of Canterbury, New Zealand, 1997.
12 Sutcliffe DJ, Yu H.S, Page AW. "Lower Bound Limit Analysis of Unreinforced Masonry Shear Walls." Computer & Structures 2001; (79):1295-1312
13 Vermeltfoort AT, Raijimakers TMJ, Jansen HJM. "Shear Test on Masonry Walls." Proceedings of 6th North American Masonry Conference, Philadelphia, 1993:1183-93.
14 IAEE."IAEE manual: Guidelines for earthquake resistant non-engineered construction." 1986